P. Purnachander Rao[1]

K. Prakash[2]

M. Suryakalavathi[3]

A Solar PV-Fed Hybrid Active Power Filter Based on I-Luo Converter for Power Quality Enhancement in Distributed Generation Systems

Journal of Electrical Systems

Abstract: - The adoption of Distributed Generation (DG) systems, such as photovoltaic (PV) panels, is increasing due to their environmental advantages and potential to lessen reliance on fossil fuels. However, Renewable Energy Sources (RES) like PV can cause Power Quality (PQ) issues, including voltage and current harmonics, which negatively impact grid stability and efficiency. To mitigate these problems, this study introduces a Hybrid Active Power Filter (HAPF). This filter, powered by a high-gain Interleaved Luo (I-Luo) Converter fed by a PV system, effectively reduces harmonic distortions, addresses reactive power issues, and stabilizes voltage in the distribution network. To further enhance the converter's performance, a Modified Squirrel Search-based PI controller is implemented. Known for its robust and efficient convergence, this optimization algorithm adjusts the PI controller settings to improve dynamic response and ensure precise harmonic compensation. Additionally, a Recurrent Neural Network (RNN)-based harmonic extraction technique is employed to accurately identify and quantify harmonic components in voltage and current waveforms, enabling precise HAPF control. Simulations conducted in MATLAB demonstrate that the integration of RNN-based harmonic extraction, HAPF, and the I-Luo Converter with Modified Squirrel Search optimization significantly enhances Power Quality in DG systems.

Keywords: Distributed Generation (DG), PV, PQ, RNN, HAPF, MSSO, I-Luo converter.

1.Introduction

As Distributed Renewable Energy Sources (RESs) are increasingly integrated into the utility grid, Power Quality of Distributed Generation systems (DGSs) have emerged as a key issue. Control methodologies and grid-connected converter architectures have been extensively studied as modules for integrating RESs into utility grids [1, 2]. Due to harmonic resonant frequencies, reactive, harmonic, and imbalanced current from local loads can exacerbate the PQ at the point of common coupling (PCC) and lead to DGS instabilities [3]. Two strategies are frequently used to address these issues. One focuses on applying state-of-the-art control techniques to improve the output current waveforms and the ability of grid-connected converters to operate continuously under atypical utility conditions [4]. This method might not be able to totally remove the DGSs' negative effects on the current poor power quality, though. The second way to deal with the power quality issue is to use particular PQ conditioners. Nevertheless, because of the unwanted resonance present in high-voltage circuits, the use of passive filters cannot guarantee desired results. Passive power filters are not as good as active power filters because of their resonance issues and inability to reduce system harmonics. In the meantime, harmonic removal with active filters is very expensive. Thus, a hybrid active filter—an intermediary solution—has been identified as the optimal choice for harmonic reduction [5-8]. In this study, we address the use of HAPF for harmonic removal in electrical distribution networks. Because it actively compensates for unwanted harmonics and reactive power components, the HAPF plays a crucial role in achieving improved PQ. The use of RNN for precise harmonic extraction is a notable innovation in this work. This method contributes to the accurate control of the HAPF by enabling the system to intelligently and adaptively extract harmonic information from voltage and current waveforms. Conversely, installing a separate device is necessary for either an active or passive air conditioner. Negative consequences such as increased cost, power rating, dimensions, and man-hour will always exist as a result. From DGSs' point of view, some grid-connected power conversion devices offer extra features like reactive power control, suppression of distortions, and changes in uneven energy that could be useful add-ons to improve PQ. DGSs constructed around electrical components have the potential to be significant players

[1*]Research Scholar, Electrical and Electronics Engineering, JNTUH, Hyderabad

[2]Professor, Electrical and Electronics Engineering, Vaagdevi College of Engineering

[3]Professor, Electrical and Electronics Engineering, JNTUH, Hyderabad

in LV network distribution by offering extra amenities to the electrical grid as a high degree method of integrating RESs. This additional facility requires knowledge of these grid-connected converters. The operation of power converters in DGSs is suggested to be either grid-feeding or grid-supporting, based on examples of hierarchical control systems [9–14].

Implementing renewable energy systems, particularly photovoltaic (PV) systems, is widely recommended. Residential PV systems are increasingly popular for several reasons. One significant factor is the substantial drop in PV costs in recent years, with expectations for further reductions. Additionally, extensive research is underway to enhance PV efficiency, indicating that PV systems will likely dominate Distributed Generation (DG) in the coming years. However, sudden increases in sunlight can cause the PV array's output current to surge, requiring the use of a converter to manage this variability[14-17].

Single-stage converters like Buck, Boost, Buck-Boost, SEPIC, and LUO converters are commonly used as DC-DC converters due to their reliability, cost-effectiveness, and simple design. However, these converters often suffer from low efficiency, high ripple, and fluctuating source and load currents.

To address these issues, Interleaved LUO (I-Luo) converters have been proposed, offering improved efficiency and reduced ripples. Traditional PI controllers, while widely used, are sensitive to parameter changes, environmental conditions, and other factors. Therefore, a more robust controller is needed to manage variables such as the fluctuating weather conditions affecting PV systems [17-21].

Among the optimization techniques that have become developed over time are PSO, P&O, and GA. All of these systems have different requirements for hardware, cost, monitoring speed, precision, and effectiveness. They often function excellently, but they are difficult to implement on a low-cost digital controller [22–25]. The well-known class of meta-heuristics known as MSSO, which takes its cue from squirrels, is used in this work. To enhance the energy flow of a grid-integrated PV system, a high gained I-Luo Converter and a PI controller based on the MSSO algorithm are used in this paper.

The study presents the Hybrid Active Power Filter (HAPF) as an essential tool for enhancing Power Quality (PQ) in distributed generation systems. The HAPF effectively reduces harmonic distortions, manages reactive power fluctuations, and stabilizes voltage, tackling PQ issues linked to the integration of Renewable Energy Sources (RESs) such as photovoltaic (PV) systems into power grids. Furthermore, the research incorporates novel methods to boost the HAPF's efficiency in maintaining grid stability and overall performance.

The proposed work includes several key innovations:

- A high-gain Interleaved Luo Converter for improved power conversion efficiency from the PV system.

- An MSSO-based PI controller for advanced control.

- An RNN-based technique for precise harmonic extraction from voltage and current waveforms, enabling adaptive and accurate HAPF control.

The proposed work advances the field of DGSs with innovative approaches to enhancing power quality. The system's effectiveness is thoroughly validated through MATLAB simulations.

2. Overview of the Proposed System

The suggested system ensures resilient operation of the PV system to meet non-linear load demands. Components like the PV array, I-Luo converter, Modified Squirrel-based PI controller, and HAPF were carefully considered in system design. Figure 1 illustrates the basic circuit design of the proposed solar PV-based system. The I-Luo converter boosts output while minimizing switching losses from the PV array. A PI controller with MSSO-tuned parameters maintains the I-Luo converter's output voltage. Through optimization, the I-Luo converter reduces switching losses and enhances output voltage stability.

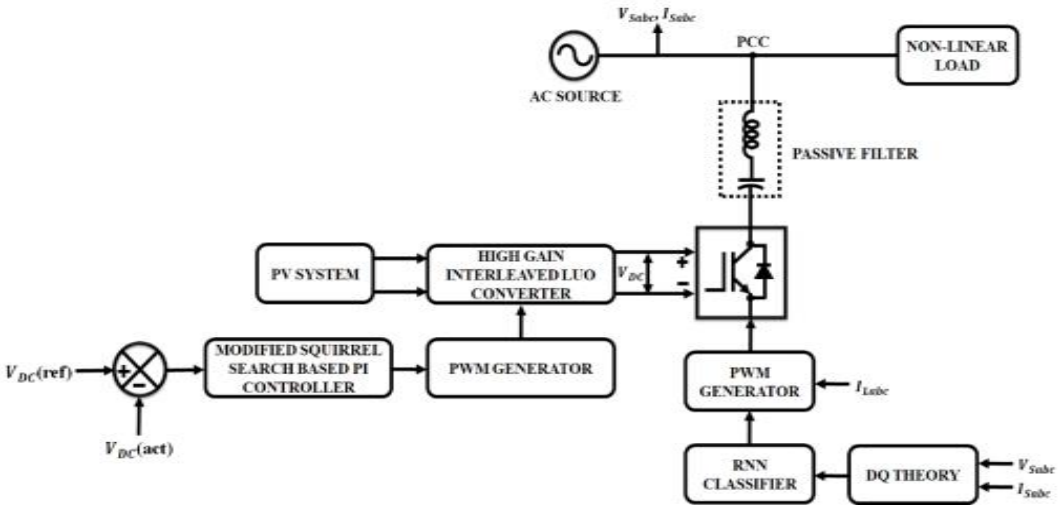

Figure 1. Basic configuration of Hybrid Active Power Filter

The MSSO-PI controller effectively addresses peak overshoot compared to the traditional PI controller. A calibrated PI controller ensures steady-state operation without exceeding set limits. Solar PV systems can surpass their rated capacities, enabling excess power to be shared with neighbouring users. Restrictions during optimization manage detuning impacts and failures, enhancing filter reliability. The HAPF, utilizing RNN, reduces harmonics and improves power factor in distribution systems. The subsequent sections detail the proposed system's architecture and implementation.

3. Modelling of the work

3.1. Design of PV Array

Figure 2 illustrates the equivalent circuit of the PV system. The PV cell's performance is influenced by its input characteristics, where I_D represents diode current, I and V denote output current and voltage, and R_p and R_s represent series and parallel resistance. The input current of the solar cell is termed as I_{PV}.

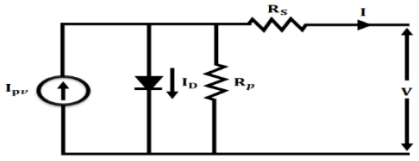

Figure 2. Equivalent circuit of PV cell

Equations (1) and (2) illustrate that PV cell's output current varies depending on the input cell current, temperature voltage, the PV cell's output voltage, and its resistance.

$$I = I_{PVcell} - I_{scell}[exp\,\frac{(qv)}{\alpha KT} - 1] \quad (1)$$

$$I = I_{PV} - I_0\left[exp\,\frac{(v+R_S.I)q}{\alpha V_k} - 1\right] - \frac{(v+R_S.I)}{R_p} \quad (2)$$

Equation (2)'s representation of current output is for a single PV cell. With the PV module arrangement, this can be expressed as (3) illustrates. Typically, this is dependent on N_s, or the quantity of PV cells linked in series.

$$I = I_{PV} - I_0\left[exp\,\frac{(v+R_S.I)q}{\alpha KT.N_s} - 1\right] - \frac{(v+R_S.I)}{R_p} \quad (3)$$

As evident from (3), the current-voltage (I-V) relationship of the PV array is non-linear due to variations in solar insolation and array temperature. Optimizing the ideal working region becomes crucial for maximizing PV output power, where matching the array resistance with the load resistance results in peak power production. The positive I-LUO converter then harnesses the recovered output power from the PV panel.

3.2. Interleaved Luo Converter

To get minimal output distortion and excellent voltage transfer efficiency of PV energy are made possible with the aid of the I-Luo converter. Figure 3 shows the converter's planned circuit. Simulink-based simulation is used to assess the I-Luo converter's efficiency under varying illumination.

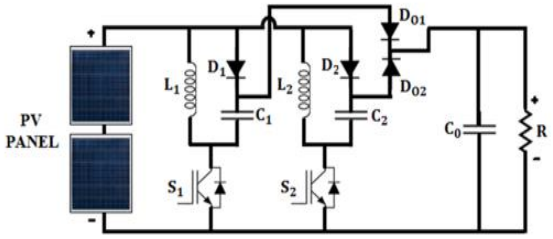

Figure 3. I-Luo converter Circuit

3.2.1 Principle of Working

This section covers the operation and performance of the I-Luo converter when it is turned ON and OFF. The detailed description of I-Luo converter operation is depicted in Figure 4 (a–c). The fundamental purpose of the I-Luo converter is to maintain steady-state voltage and current. The power switch S_1 and S_2 , the switching capacitor C_1 and C_2 , and the inductance L_1 and L_2 are all depicted as parts of the converter.

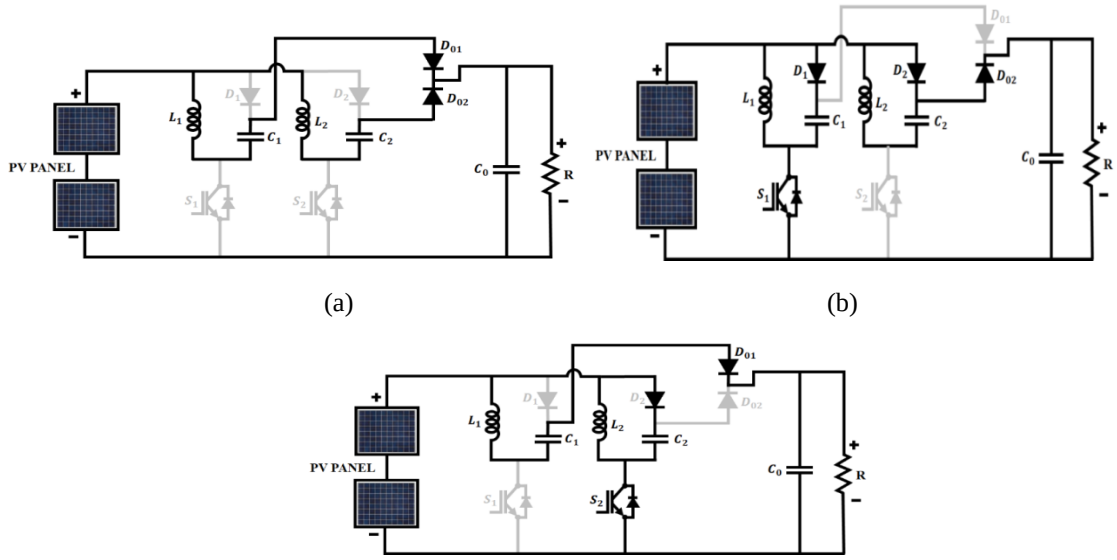

Figure 4. Working of the I-Luo converter in: (a) Mode-1; (b) Mode-2 and 4; (c) Mode-3

Power switches S_1 and S_2 are firstly in the ON and OFF positions in mode-1, respectively, which causes diode D_{01} to be forward biased and D_{02} to be reverse biased. The extra PV supply charges the capacitors C_1 and C_2 while leaving the inductors L_1 and L_2 contacts open so as to permit current to pass through the load. The converter that has been recommended contains two diodes. It regulates the current in one-way switches. Here, the reverse-biased diode D_2 limits the source of current from the other side whereas the forward-biased diode D_1 permits a supply of current across the load. mode-2 demonstrates that the diodes D_{01} and D_{02} are reverse biased as a result of the power switches S_1 and S_2 remaining in the ON state simultaneously. At this point, the PV supply is charging the inductor L_1 , L_2 . In mode-2, it is discovered that both diodes D_1 and D_2 are reverse biased. Power switches S_1 and S_2 are in the OFF and ON states at the start of mode- 3. As a result, diode D_{01} is forward biased and diode D_{02} is reverse biased. L_2 is released once L_1 has been charged, allowing flow of current to the load. While diode D_1 limits, diode D_2 allows current to move in the direction of the load. Mode-4

demonstrates that both power switches are in OFF, which indicates the forward bias for diodes D_{01} and D_{02}. The load releases the mode-4 inductor, placing the diode in forward bias.

Equation 4 expresses the converter's output voltage, which is V_0 .

$$V_0 = 3\frac{2-d}{1-d}V_{PV} \quad (4)$$

Where V_{PV} ,the PV array's output voltage and d is the converter's duty cycle. If the PV's output voltage is at its lowest, a high operating cycle might be required. A power switch, a capacitor, and an inductor make up the I-Luo converter. Equation (5) illustrates that only 40% of ripple current can be allowed when an inductor is used. As a result, the issue of output ripple current can be reduced.

$$\Delta I_L = I_L \times 40\% = I_0 \frac{(V_0 \times 40\%)}{V_{PV}(\min)} \quad (5)$$

The nominal values of L_1 and L_2 can be calculated using (6) as follows:

$$L_1, L_2 = \frac{V_{PV}(\min)}{\Delta I_L \times f_{sw}} . dmax \quad (6)$$

where $dmax$ represents the pulse's highest duty cycle when applied to an I-Luo converter. Equation (7) can be used to get the current's input RMS value:

$$I_{Cin}(rms) = \frac{\Delta I_L}{\sqrt{12}} \quad (7)$$

As demonstrated in (8), the output current is instantly transferred to the output capacitor when the Switch is ON, electrifying the inductor.

$$I_{C0}(rms) = I_0\sqrt{\frac{V_{DC}+V_D}{V_{PV}(\min)}} \quad (8)$$

where V_D is the voltage drop between diodes D_1 and D_{01} and V_{DC} is the converter's output voltage. Equation (9), which gives the resulting capacitance value, can be used to calculate it.

$$C_0 = \frac{I_0 \times d}{V_{ripple} X_{0.5} X_{fsw}} \quad (9)$$

where $X_{0.5}$ and X_{fsw} are the impedance at 50% duty cycle and switching frequency, respectively, and d is the PWM pulse duty cycle.

3.3. Tuning of PI Controller with Modified Squirrel Search Optimization (MSSO) Algorithm

The MSSO, a ground-breaking optimization method, assumes that the search region contains (n) squirrels that fly and (n) deciduous trees. Each flying squirrel only has one tree, and they search through them in order. Three sorts of tree types are distinguished: normal, oak or acorn nuts, and hickory. The final assumption is that three of the trees and one of the trees is an oak tree. The following definition describes the location vector for each *ith* flying squirrel.

$$Fs_i = (Fs_{i1}, Fs_{i2}, \dots, Fs_{id}), (i = 1,2, \dots, n) \quad (10)$$

Every flying squirrel's size is Fs_{ij} , and its beginning location is

$$Fs_i = Fs_L + U(0,1) * Fs_U - Fs_L \quad (11)$$

Where U(0,1) is a value chosen at random from [0, 1] and Fs_U, Fs_L are the upper and lower search boundaries. The fitness values for the people will be arranged in ascending order, with hickory trees serving as the least value, followed by acorn trees on the other three minimum numbers, and normal trees for the remaining trees. Predators in the forest have a Pdp probability of being there, which affects how individuals migrate to locate food. If there are no predators in the forest, there are three categories for how individuals find food:

$$FS_{at}^{t+1} = \begin{cases} FS_{at}^{t} + d_g * G_c * FS_{ht}^{t} - FS_{at}^{t})R_1 \geq Pdp \\ Random\ Location\ others \end{cases} \quad (12)$$

R_1 is a random number between [0,1] utilized to maintain equilibrium between the exploration and exploitation modes. Flying squirrels will transition from conventional trees to acorn trees, taking the following new position:

$$FS_{nt}^{t+1} = \begin{cases} FS_{nt}^{t} + d_g * G_c * FS_{at}^{t} - FS_{nt}^{t})R_2 \geq Pdp \\ Random\ Location\ others \end{cases} \quad (13)$$

R_2 has a value drawn at random from [0, 1]. Flying squirrels may transition from hickory trees to conventional trees, changing their location to:

$$FS_{nt}^{t+1} = \begin{cases} FS_{nt}^{t} + d_g * G_c * FS_{ht}^{t} - FS_{nt}^{t})R_3 \geq Pdp \\ Random\ Location\ others \end{cases} \quad (14)$$

R_3 also has a random value in the [0, 1] range. The gliding distance and angle are shown in (21) as follows:

$$d_g = \frac{h_g}{\tan(\varphi) * sf} \quad (15)$$

$$\tan(\varphi) = \frac{D}{L} \quad (16)$$

$$D = \frac{1}{2\rho V^2 S C_D} \quad (17)$$

$$D = \frac{1}{2\rho V^2 S C_L} \quad (18)$$

$$S_t^t = \sqrt{\sum_{k=1}^{D} S_{ai,k}^{t} - S_{h,k}^{t}\ \ i = 1,2,\ldots.,Nfs} \quad (19)$$

Some squirrels couldn't find food at the conclusion of the winter season, so they had to look in other places. These squirrels moved as shown in (20),

$$FS_{inew}^{t+} = Fs_L + Levy(n) * (Fs_U - Fs_L) \quad (20)$$

$$\text{Where } Levy(n) = 0.01 * \frac{r_2 \sigma}{|r_b|^{\frac{1}{\beta}}} \quad (21)$$

(n) = (n 1), r_a and r_b are two random numbers between [0, 1], and is a constant value of 1.5. Last but not least, in order to get the best system efficiency, it is necessary to choose a suitable set of fitness criteria. The MSSO method uses the ITAE in (22) as a measure of fitness parameter.

$$ITA = \int |e|\, dt \quad (22)$$

Once the squirrels' locations are updated based on migration and possible Levy Flight, the algorithm calculates the control efforts for each squirrel. This entails computing the error between the reference and actual voltages, followed by generating proportional and integral terms using the PI controller's gains. The resultant control effort represents an adjustment to the converter's switching operation. The application of calculated control efforts to the Interleaved Luo Converter induces adjustments in its switching logic. This dynamic adaptation of the switching operation aims to steer the actual output voltage closer to the desired reference voltage.

3.4. Modelling of Hybrid Active Power Filter

In Figure 5, an active filter and passive filter combine to form a HAPF, controlled by a dedicated block. While the active filter addresses low-frequency harmonics from non-linear loads, the passive filter tackles higher-frequency harmonics. HAPF offers advantages over traditional filters by addressing nearby harmonic current issues and resonances, at a lower capacity compared to regular active power filters. Employing HAPF provides a cost-effective solution for active filter implementation. Selection criteria for HAPF effectiveness include filter structure, control strategy (e.g., RNN), filter type in the control loop, and component sizing.

3.4.1. DQ Theory based control using RNN Classifier

The DQ theory, also known as Park's or Clarke's transformation, converts three-phase signals into two orthogonal components: D (Direct) and Q (Quadrature), simplifying control in rotating reference frames. In HAPF control, it's utilized to extract harmonic components from three-phase currents, generating reference currents for desired harmonic compensation and power factor correction. Figure 5 illustrates the structure of RNN-assisted DQ control. Transformation equations for DQ theory are outlined below:

D-axis component (i_d):

$$i_d = i_a * cos(\theta) + i_b * cos(\theta - 2\pi/3) + i_c * cos(\theta + \frac{2\pi}{3}) \quad (23)$$

Q-axis component (i_q):

$$i_q = -i_a * sin(\theta) - i_b * sin(\theta - 2\pi/3) - i_c * sin(\theta + 2\pi/3) \quad (24)$$

Where: i_a, i_b, i_c are the measured three-phase currents. θ is the angle of the rotating reference frame.

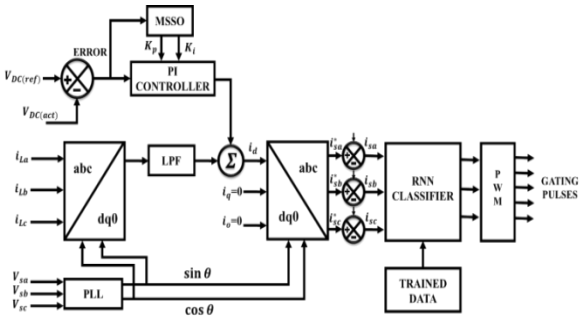

Figure 5. DQ Theory based control

The RNN classifier is a trained intelligent system designed to detect and remove harmonics from the reference current signal, generating a distortion-free output. The process involves several steps: assembling a comprehensive dataset with labelled reference current signals, covering various operational conditions and harmonic interferences. During training, the RNN learns intricate patterns distinguishing harmonics from non-harmonics within the signals. Sequentially presented input signals enable the RNN to progressively analyze and understand sequential dependencies, making predictions about harmonic presence.

During training, a defined loss function quantifies the disparity between the RNN's predictions and actual labels (harmonic or non-harmonic). An optimization algorithm refines the RNN's predictive abilities by adjusting internal parameters. Once trained, the RNN processes new reference current signals in real-time, continually predicting harmonics. Upon identifying harmonics, the RNN adjusts the output to eliminate harmonic content, resulting in an improved reference current. This distortion-free signal serves as an optimal input for the PWM generator, controlling the Hybrid Active Power Filter (HAPF).

4. Results and Discussions

Solar cell power is enhanced via an I-Luo converter before conversion to AC power using a single-phase VSI system in MATLAB. The parameter Specifications for the proposed system are:

PV system: Pak Power 10KW, $V_{OC} = 22.6V, I_{SC} = 41.6A, V_{SC} = 12V$, Number of panels=20,500w;

I-Luo converter: $L_1, L_2 = 1mH$, $C_1, C_2 = 4.7\mu F$, $C_0 = 22{,}00\mu F$ and the Non-Linear load R= 100Ω L =10mH.

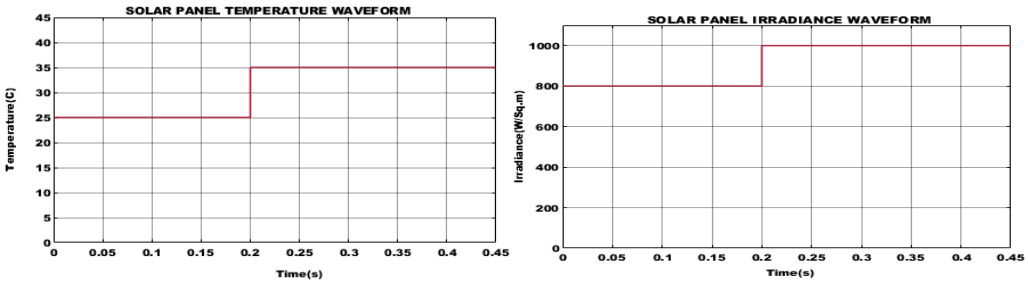

(a) (b)

Figure 6. Solar panel (a) Temperature waveform (b) Irradiance waveform

Figure 6 illustrates the characteristics of the solar PV system concerning temperature and radiation. Following the sun's temperature rise, the initial 25°C temperature increases to an average of 35°C. Similarly, the panel maintains its initial irradiation level of 800W/sq m, but after 0.2s, it rises to 1000W/sq m due to temperature increase, supplying ample power to the converter input.

Figure 7 illustrates the waveform of electrical voltage and current from the solar panel to the I-Luo converter. Initially, an input voltage of 62V is achieved and maintained for 0.2 seconds. Subsequently, the voltage increases to 75V and remains constant due to a rise in the PV parameter. Consequently, a constant current level of 80A is reached after 0.22 seconds from the peak increase of the PV current's first phase.

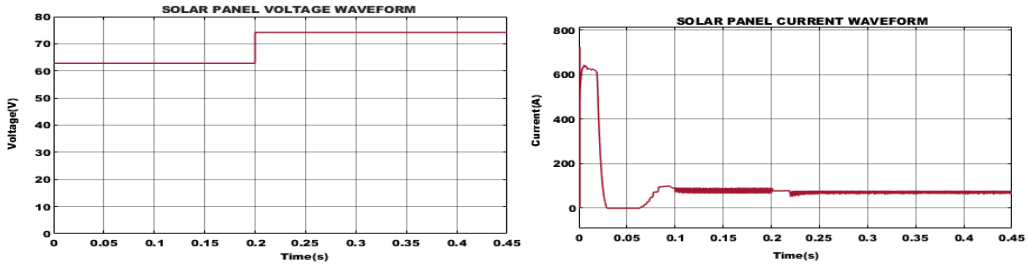

(a) (b)

Figure 7. Solar panel (a) Voltage waveform (b) Current waveform

Figure 8 illustrates the control of the DC link supply to achieve the output voltage of the I-Luo converter using PI and MSSO-PI controllers. In Figure 8(a), it is evident that tuning is necessary as the PI controller fails to stabilize the voltage at 600V. Conversely, Figure 8(b) shows that the MSSO-tuned PI controller produces a reliable output. To promptly attain stable DC voltage and maintain a stabilized voltage of 600V, the use of an MSSO-PI controller is recommended.

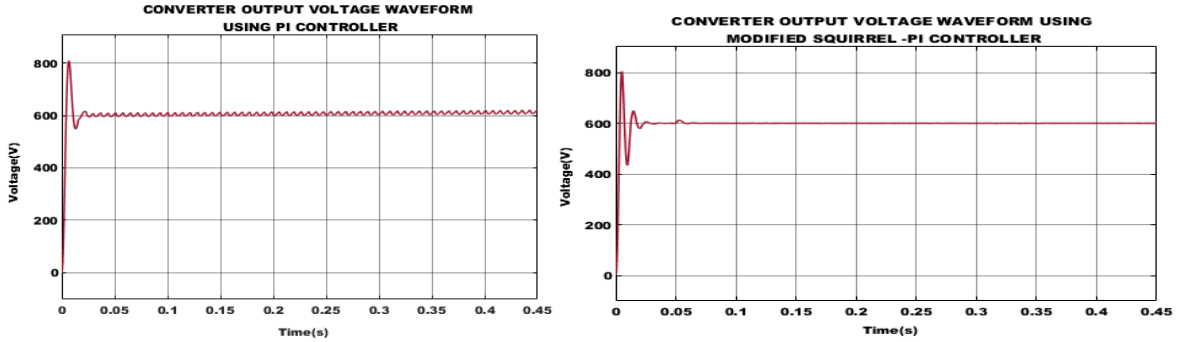

(a) (b)

Figure 8. Output Voltage of Proposed Converter by adopting (a) PI controller, (b) MSSO-PI controller

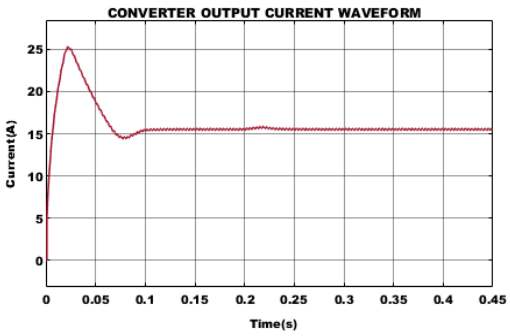

Figure 9. Converter Output Current

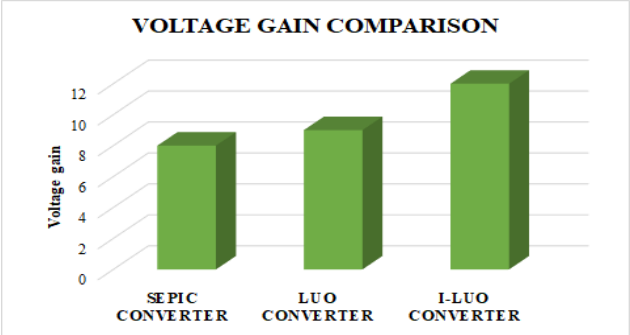

Figure 10. Comparison of Voltage gain

The suitable output current from the I-Luo converter is shown in Figure 9. The current is observed to vary in the initial phases before stabilizing and remaining constant at 16A after 0.1s.

Figure 10 illustrates a voltage gain analysis comparing the proposed I-Luo converter architecture to conventional converters. Investigations revealed that the proposed converter produced a 1:12 improvement in voltage gain.

Table 1: Comparison of Converter Performance

Converters	**Voltage gain**	**Efficiency (%)**
SEPIC	1:8	88.82 % [26]
Luo	1:9	90% [27]
I-Luo	1:12	97.42%

Table 1 presents a comparison of the effectiveness of the proposed converter with conventional SEPIC and Luo converters. The recommended I-Luo converter architecture demonstrates superior performance with 97.42% efficiency and a 1:12 voltage gain compared to SEPIC and Luo converter architectures. This information suggests that the PV system efficiently raises the low DC voltage generated by solar panels to an optimal level compatible with grid integration.

Table 2: Controller Performance Analysis

Performance Measures	**PI**	**MSSO-PI**
Peak Time (T_p) in sec	0.02	0.002
Rise Time (T_r) in sec	0.002	0.001
Settling Time (T_s) in sec	0.45	0.07

Table 2 displays the outcomes of modifying the PI controller variables to provide better converter performance along with the related findings. The recommended MSSO-PI controller, as seen in Figure 9, stabilizes a voltage of 600V faster than the conventional PI controller at a time of 0.01s. As a result, the suggested system reacts to changes in operational conditions, such as fluctuating solar irradiance, load requirements, and grid conditions, promptly and precisely.

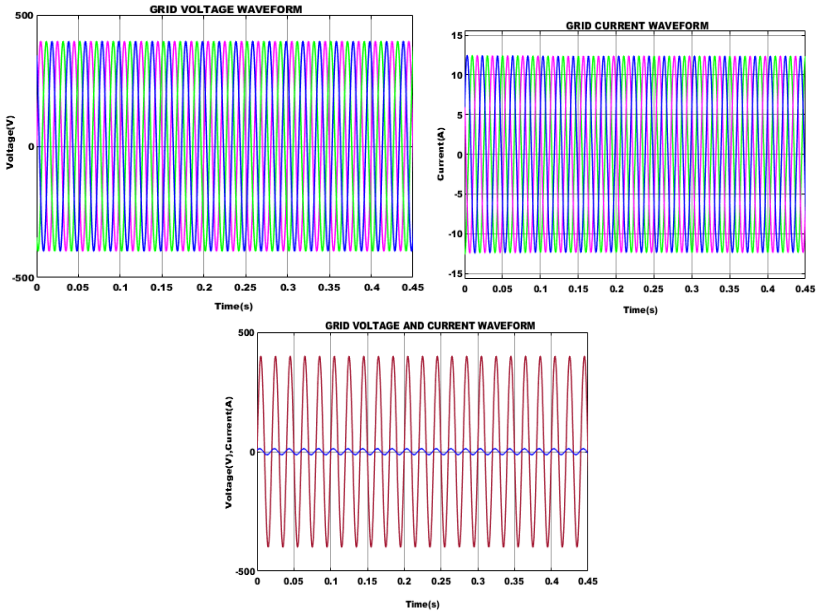

(a) (b) (c)

Figure 11. 3-Φ Grid (a) Voltage and (b) Current (c) Voltage and Current

Figures 11(a) and (b) display the voltage and current waveforms of a 3Φ grid, representing various forms of electrical energy. These waveforms ensure consistent power transmission, efficient operation of electrical equipment, and maintenance of system reliability through regulated voltage and current flow.

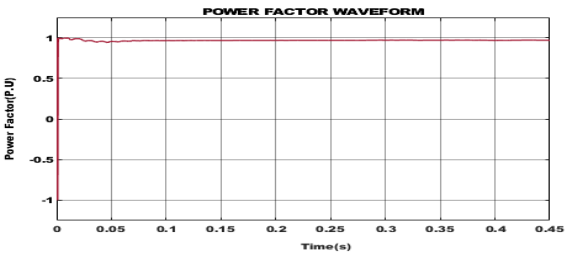

Figure 12. Power factor waveform

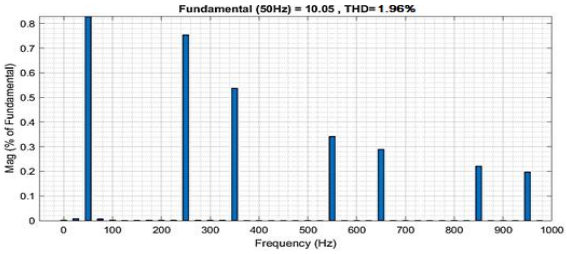

Figure 13. Performance measure of THD value

Figure 12 illustrates that the system's power factor is close to unity, while Figure 13 analyses the effectiveness of THD in the grid-connected PV system, showing a value of 1.96%. This indicates that the PV system generates high-quality, pure power with minimal harmonic distortion fed into the grid. Moreover, it ensures enhanced grid compatibility, reducing the risk of breakdowns and instabilities.

5. Conclusion

The increasing use of nonlinear devices introduces harmonics into power system networks, causing distortion in current and voltage signals and harm to power distributed Generation systems (DGS). Therefore, eliminating harmonics in power systems is crucial. HAPF based on RNN provides an effective and economical solution to reduce harmonics and enhance power factor in DGS. For power factor (PF) re-regulation at the mains in steady state and varying operational voltages, an I-Luo converter for PV systems is devised, and PI controller settings are adjusted using the MSSO. Simulation results demonstrate a steady and efficient response for the suggested controller, achieving the target speed with a quick and stable reaction. THD effectiveness achieves 1.96%, indicating minimal harmonic distortion entering the grid.

References

[1] S. Zhou et al., "An Improved Design of Current Controller for LCL-Type Grid-Connected Converter to Reduce Negative Effect of PLL in Weak Grid," in IEEE Journal of Emerging and Selected Topics in Power Electronics, June 2018; vol. 6, no. 2, pp. 648-663.

[2] D.-M. Phan and H. -H. Lee, "Interlinking Converter to Improve Power Quality in Hybrid AC–DC Microgrids With Nonlinear Loads," in IEEE Journal of Emerging and Selected Topics in Power Electronics, Sept. 2019; vol. 7, no. 3, pp. 1959-1968.

[3] S. Liu, X. Wang and P. X. Liu, "A Stochastic Stability Enhancement Method of Grid-Connected Distributed Energy Storage Systems," in IEEE Transactions on Smart Grid, Sept. 2017; vol. 8, no. 5, pp. 2062-2070.

[4] M. R. Elkadeem, M. Abd Elaziz, Z. Ullah, S. Wang and S. W. Sharshir, "Optimal Planning of Renewable Energy-Integrated Distribution System Considering Uncertainties," in IEEE Access, 2019; vol. 7, pp. 164887-164907.

[5] B. N. Rao, Y. Suresh, A. K. Panda, B. S. Naik and V. Jammala, "Development of cascaded multilevel inverter based active power filter with reduced transformers," in CPSS Transactions on Power Electronics and Applications, June 2020; vol. 5, no. 2, pp. 147-157.

[6] P. K. Ray, "Power quality improvement using VLLMS based adaptive shunt active filter," in CPSS Transactions on Power Electronics and Applications, June 2018; vol. 3, no. 2, pp. 154-162.

[7] S. C. Ferreira, R. B. Gonzatti, R. R. Pereira, C. H. da Silva, L. E. B. da Silva and G. Lambert-Torres, "Finite Control Set Model Predictive Control for Dynamic Reactive Power Compensation With Hybrid Active Power Filters," in IEEE Transactions on Industrial Electronics, March 2018; vol. 65, no. 3, pp. 2608-2617.

[8] S. Devassy and B. Singh, "Control of a Solar Photovoltaic Integrated Universal Active Power Filter Based on a Discrete Adaptive Filter," in IEEE Transactions on Industrial Informatics, July 2018; vol. 14, no. 7, pp. 3003-3012.

[9] M. E. Raoufat, A. Khayatian and A. Mojallal, "Performance Recovery of Voltage Source Converters With Application to Grid-Connected Fuel Cell DGs," in IEEE Transactions on Smart Grid, March 2018; vol. 9, no. 2, pp. 1197-1204.

[10] H. Bizhani, R. Noroozian, S. M. Muyeen, K. Techato and F. Blaabjerg, "A Grid-Connected Smart Extendable Structure for Hybrid Integration of Distributed Generations," in IEEE Access, 2019; vol. 7, pp. 105235-105246.

[11] S. Kewat and B. Singh, "Grid Synchronization of WEC-PV-BES Based Distributed Generation System Using Robust Control Strategy," in IEEE Transactions on Industry Applications, 2020; vol. 56, no. 6, pp. 7088-7098.

[12] B. Zaker, G. B. Gharehpetian and M. Karrari, "A Novel Measurement-Based Dynamic Equivalent Model of Grid-Connected Microgrids," in IEEE Transactions on Industrial Informatics, vol. 15, no. 4, pp. 2032-2043, April 2019.

[13] A. Rodríguez-Cabero, M. Prodanovic and J. Roldán-Perez, "Analysis of Dynamic Properties of VSCs Connected to Weak Grids Including the Effects of Dead Time and Time Delays," in IEEE Transactions on Sustainable Energy, vol. 10, no. 3, pp. 1066-1075, July 2019.

[14] P. Wang, W. Wang and D. Xu, "Optimal Sizing of Distributed Generations in DC Microgrids With Comprehensive Consideration of System Operation Modes and Operation Targets," in IEEE Access, vol. 6, pp. 31129-31140, 2018.

[15] S. Singh, S. Kewat, B. Singh, B. K. Panigrahi and M. K. Kushwaha, "Seamless Control of Solar PV Grid Interfaced System With Islanding Operation," in IEEE Power and Energy Technology Systems Journal, vol. 6, no. 3, pp. 162-171, Sept. 2019.

[16] A. A. Abdelsalam, A. A. Salem, E. S. Oda and A. A. Eldesouky, "Islanding Detection of Microgrid Incorporating Inverter Based DGs Using Long Short-Term Memory Network," in IEEE Access, vol. 8, pp. 106471-106486, 2020.

[17] A. Verma, R. Krishan and S. Mishra, "A Novel PV Inverter Control for Maximization of Wind Power Penetration," in IEEE Transactions on Industry Applications, vol. 54, no. 6, pp. 6364-6373, Nov.-Dec. 2018.

[18] D. Chen and H. Zeng, "A Buck Type Multi-Input Distributed Generation System With Parallel-Timesharing Power Supply," in IEEE Access, vol. 8, pp. 79958-79968, 2020.

[19] S. Singh, S. Kewat, B. Singh, B. K. Panigrahi and M. K. Kushwaha, "Seamless Control of Solar PV Grid Interfaced System With Islanding Operation," in IEEE Power and Energy Technology Systems Journal, vol. 6, no. 3, pp. 162-171, Sept. 2019.

[20] Tavakoli, Saman Dadjo, Mohammad Mahdavyfakhr, Mohsen Hamzeh, Keyhan Sheshyekani, and Ebrahim Afjei. "A unified control strategy for power sharing and voltage balancing in bipolar DC microgrids." Sustainable Energy, Grids and Networks ,Vol. 11 , pp: 58-68,2017.

[21] Faridpak, Behdad, Meisam Farrokhifar, Mojtaba Nasiri, Arman Alahyari, and Nasser Sadoogi. "Developing a super-lift luo-converter with integration of buck converters for electric vehicle applications." CSEE Journal of Power and Energy Systems ,Vol.7, no. 4 ,pp: 811-820,2020.

[22] A. K. Mishra, S. R. Das, P. K. Ray, R. K. Mallick, A. Mohanty and D. K. Mishra, "PSO-GWO Optimized Fractional Order PID Based Hybrid Shunt Active Power Filter for Power Quality Improvements," in IEEE Access, vol. 8, pp. 74497-74512, 2020.

[23] T. A. Jumani, M. W. Mustafa, A. S. Alghamdi, M. M. Rasid, A. Alamgir and A. B. Awan, "Swarm Intelligence-Based Optimization Techniques for Dynamic Response and Power Quality Enhancement of AC Microgrids: A Comprehensive Review," in IEEE Access, vol. 8, pp. 75986-76001, 2020.

[24] T. A. Jumani, M. W. Mustafa, A. S. Alghamdi, M. M. Rasid, A. Alamgir and A. B. Awan, "Swarm Intelligence-Based Optimization Techniques for Dynamic Response and Power Quality Enhancement of AC Microgrids: A Comprehensive Review," in IEEE Access, vol. 8, pp. 75986-76001, 2020.

[25] A. Selim, S. Kamel, A. S. Alghamdi and F. Jurado, "Optimal Placement of DGs in Distribution System Using an Improved Harris Hawks Optimizer Based on Single- and Multi-Objective Approaches," in IEEE Access, vol. 8, pp. 52815-52829, 2020.

[26] Javeed, Patan, Lochan Krishna Yadav, P. Venkatesh Kumar, Ranjit Kumar, and Shakti Swaroop, "SEPIC Converter for Low Power LED Applications," In Journal of Physics: Conference Series, vol. 1818, no. 1, p. 012220. IOP Publishing, 2021.

[27] P. Purnachander Rao, K. Prakash, M. Suryakalavathi, **"**Enhancing Power Quality in Distributed Generation Systems through Hybrid Active Power Filtering and Intelligent Control, " SSRG International Journal of Electrical and Electronics Engineering**,** Volume 11 Issue 4, 25-35, April 2024**.**